Electronic Supplementary Information:

Electrochemical reduction of CO_2 in organic solvents catalyzed by MoO_2

Yeonji Oh, Heron Vrubel, Sébastien Guidoux, and Xile Hu*

Laboratory of Inorganic Synthesis and Catalysis, Institute of Chemical Sciences and Engineering,

Ecole Polytechnique Fédérale de Lausanne (EPFL), Lausanne, CH 1015, Switzerland.

E-mail: xile.hu@epfl.ch

Experimental Details

Materials

Molybdenum (IV) Oxide (>99%), platinum wire (0.5 mm, 99.99%), silver wire (0.5 mm, 99.9%) and lithium perchlorate (99.99%) were purchased from Sigma Aldrich. Acetonitrile (≥99.5%) was from Merck and molybdenum rod (4.0 mm, 99.95%) was obtained from Advent Research Materials Ltd. Lead (powder type, >97%), tetrabutylammonium perchlorate (for electrochemical analysis, ≥99.0%) and tetrabutylammonium hexafluorophosphate ($TBAPF_6$) was purchased from Fluka (for electrochemical analysis, ≥99.0%).

Scanning electron microscopy (SEM) and powder x-ray diffraction (PXRD)

SEM secondary electron (SE) images were taken in a Phillips (FEI) XLF-30 FEG scanning electron microscope (Figure S1). PXRD measurements were carried out on an X'Pert Philips diffractometer using a Cu Kα radiation source (0.1540 nm). Figure S2 shows a PXRD pattern for the MoO_2 bulk powder in the 2θ range of 20°–65°. The diffraction peaks at 26.1°, 37.1°, 53.6° and 60.1° correspond respectively to the (0 1 1), (2 1 1), (0 2 2) and (0 3 1) lattice planes of the monoclinic MoO_2 crystal with lattice constants $a = 0.5620(0)$ nm, $b = 0.4860(0)$ nm, $c = 0.5630(0)$ nm and $\beta = 120.94$.[1] Peak of Mo of body centric cubic (bcc) structure is also observed. No peaks of any other phases or impurities were observed from the PXRD patterns, indicating the high purity of monoclinic MoO_2.

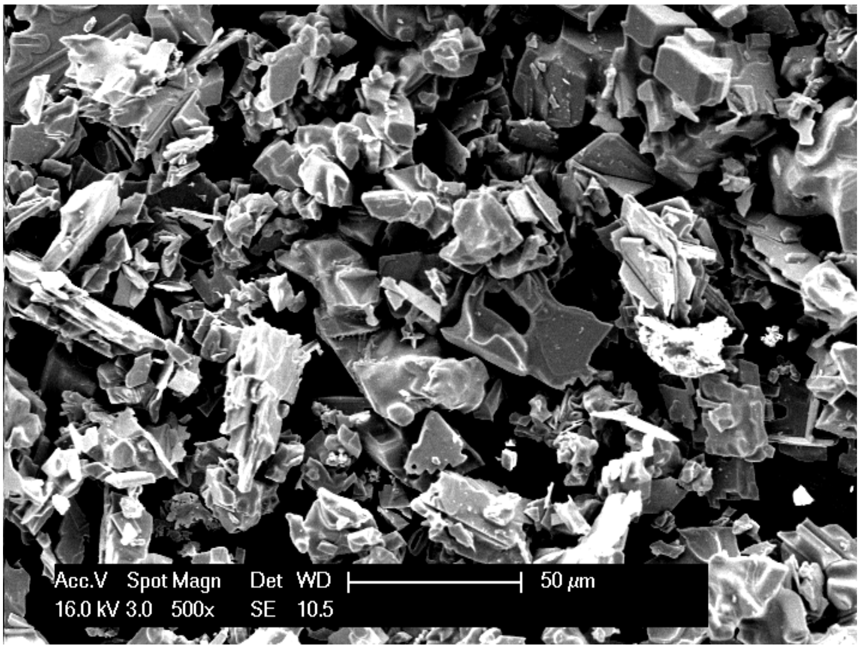

Figure S1. SEM image of the MoO_2 particles.

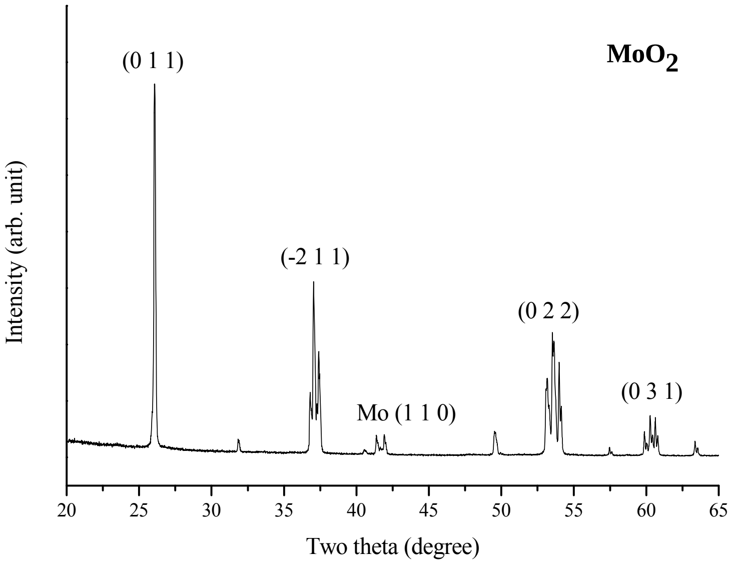

Figure S2. Powder X-ray diffraction pattern of the MoO_2 particles.

Preparation of modified MoO_2-Pb electrodes

Pb pellet has been chosen as a substrate for the working electrode. The surface of bulk Pb was cleaned by chemical etching in 50 % acetic acid then ultrasonically washed in deionized water before use. Pb was first pelletized by the pressure of 5 bar and then a thin layer of powdered catalyst (MoO_2 : Pb = 2 : 8 weight ratio) was spread on one side of the pellet. The whole set was pelletized under 10 bar to make a contact between the powdered catalyst and Pb substrate. This modified-pellet was used as a working electrode and a copper wire was connected on the back of the pellet by soldering to make an electrical contact. The contact area of the copper wire with the soldering site was isolated from the solution using molten polypropylene.

Polarization measurements (Linear sweep voltammetry)

All electrochemical measurements were recorded by a Gamry Instruments Reference 3000. Double layered glass cell with five-necks was used and the temperature was controlled by a cooling machine which makes a flow of isopropyl alcohol on the surface of the cell. A platinum wire was used as an auxiliary electrode and an Ag/Ag^+ ($AgNO_3$ (10 mM) in 0.1 M $TBAPF_6$-MeCN) electrode was used as a reference electrode. The Ag/Ag^+ reference electrode was separated by a porous Vycor tip and a Pt wire counter electrode was separated by a glass frit. Ferrocene (Fc, ABCR, ≥99.0%) was used as an internal standard and the Ag/Ag^+ reference electrode had a potential of -0.11 V vs. Fc/Fc^+ couple.[2, 3] All potentials reported here vs. Fc/Fc^+ were converted by adding -0.11 V to the potentials measured vs. the Ag/Ag^+ electrode. Initially polarization curves for the modified electrode were carried out under an inert N_2 (gas) atmosphere. After it, the solution was purged with CO_2 (Carbagas, 99.998%) for 60 min (CO_2 saturated MeCN) and the electrocatalytic CO_2 reduction was measured. It is noted that the purse of CO_2 does not lead to a significant evaporation of MeCN at -20°C.

Potentiostatic electrolysis

The potentiostatic measurements were carried out at room temperature (RT) and -20 °C. 100 mL of the electrolyte solution was used in the electrolysis experiments. When the internal temperature of the solution was verified with the aid of a thermometer, CO_2 gas was purged for 60 min prior to the electrolysis. The electrode setup was identical to that of the polarization measurements as described above. After the electrolysis, a small fraction of the cell's head space (2 mL) was sampled by gas tight syringe and analyzed by gas chromatography.

Gas chromatography, Ion Chromatography and the calculation of current efficiency

Gas chromatography measurements were conducted on a home-built GC with a TCD detector (Valco Instruments CO. Inc.) and a HayeSep DB 100/120 mesh packed column (Agilent) with argon (Ar) as a carrier gas. Calibration with different CO volume in the fixed volume of the head space was done. Since the amount of CO dissolved in 0.1 M $TBAPF_6$/MeCN at -20 °C is not known, calibration was performed with the same cell assembly as for the actual experiments. First CO_2 gas was purged for 30 min through the solution and the pressure of the head space in the cell was maintained at 1 atm. When the solution was saturated with CO_2, a 1 mL aliquot of CO gas was injected into the head space which was then allowed to stir for 30 min to equilibrate the system. After the addition of each aliquot, a small fraction of the cell's head space (2 mL) was analyzed by GC. Hence the area of the CO peak in the gas chromatogram was determined after the injection of 1, 2, 3, 4 and 5 mL of CO. This procedure was repeated more 10 times for each aliquot of CO and between these results only the most 3 reliable data without O_2 detection were chosen for the calibration. Detected O_2 indicates a gas leak in the cell. The mean values of the respective CO area were plotted against the injected CO volumes and the points were fitted linearly. The obtained calibration curve is shown in Figure S3 with its linear equation.

$$y = 6385.833\ x + 1171.367$$

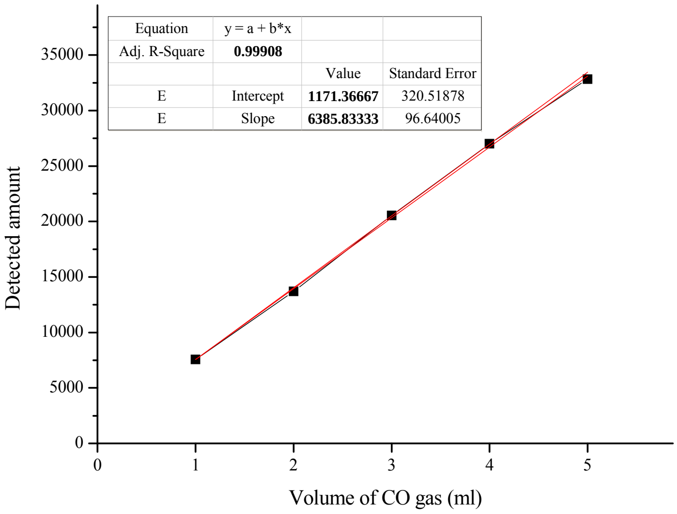

Figure S3. Calibration curve for the total amount of CO in the electrolysis cell.

With the transformed equation;

$$V_{co}\ (\mathrm{mL}) = \frac{\text{Area of detected CO - 1171.367}}{6385.833}$$

the amount of produced CO during an electrolysis experiment can directly determined with the detected area of CO peak from GC analysis. After the electrolysis, the current efficiency of an electrolysis experiment was calculated as follows. The total transferred charge (C) was divided by the Faraday constant (96485 C/mol) as well as by the factor of two, because two electrons are needed to form one CO molecule from CO_2. This gave the theoretical numbers of CO moles, considering 100% of yield. The number of moles of produced CO (derived from GC analysis) was then divided by the number of CO theoretically obtained. Multiplication of this result by 100% expressed the current efficiency as a percentage. The yield of H_2 was calculated in the same method. The liquid-phase products were analyzed and quantified by ion chromatography (Metrohm IC, Switzerland) at the end of the electrolysis. All samples were diluted 10 fold into water. The calibration for quantification of the liquid product and the calculation of current efficiency were performed in the same method as gas chromatography.

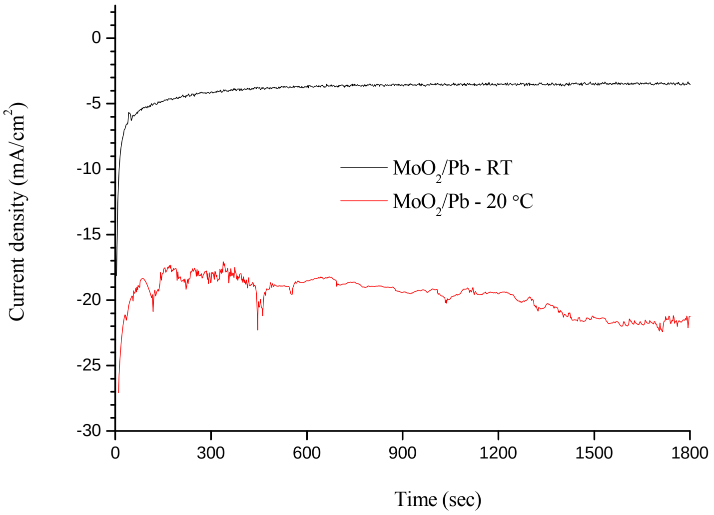

Figure S4. Potentiostatic electrolysis of the MoO$_2$/Pb at -2.45 V vs. Fc/Fc$^+$ in MeCN during 1800 sec under CO$_2$.

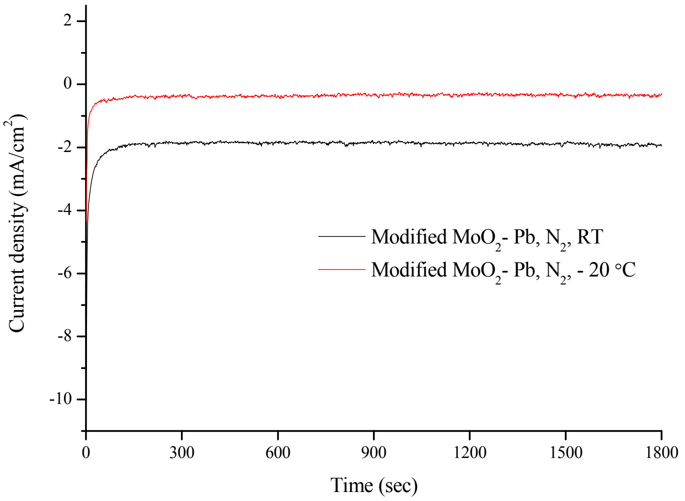

Figure S5. Potentiostatic electrolysis of the MoO$_2$/Pb electrode at -2.45 V vs. Fc/Fc$^+$ in MeCN under N$_2$ during 1800 sec.

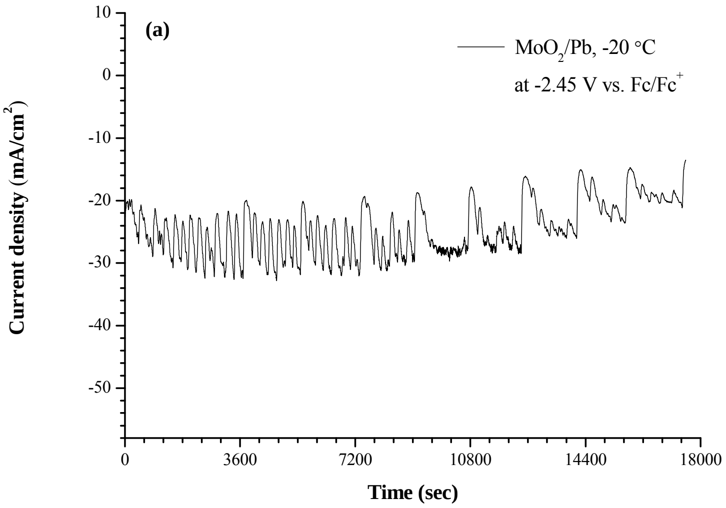

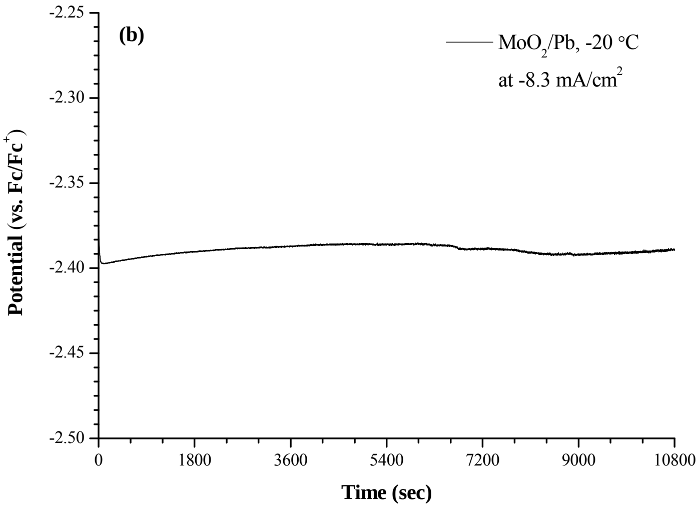

Figure S6. (a) Potentiostatic electrolysis of CO_2 reduction during 5 hours with a MoO_2/Pb elelctrode at -2.45 V vs. Fc/Fc^+ in MeCN at -20°C. (b) Galvanostatic electrolysis of CO_2 reduction during 3 hours with a MoO_2/Pb electrode at -8.3 mA/cm^2 in MeCN at -20°C.

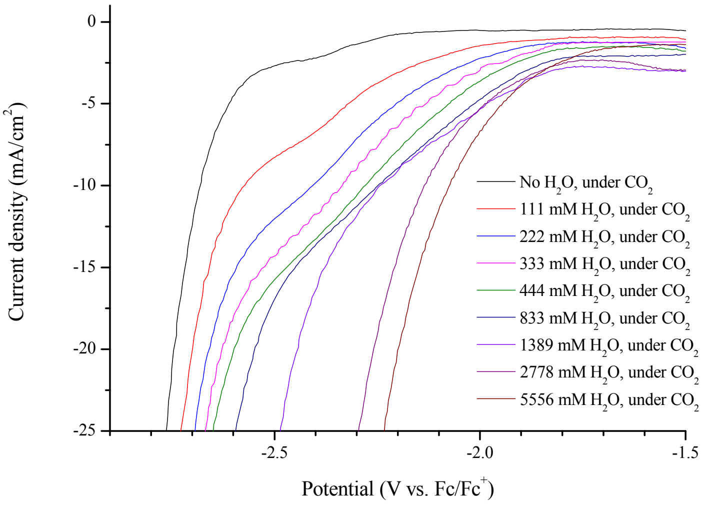

Figure S7. Polarization curves of a MoO_2/Pb electrode in CO_2-saturated MeCN with added water at RT; scan rate: 50 mV/s.

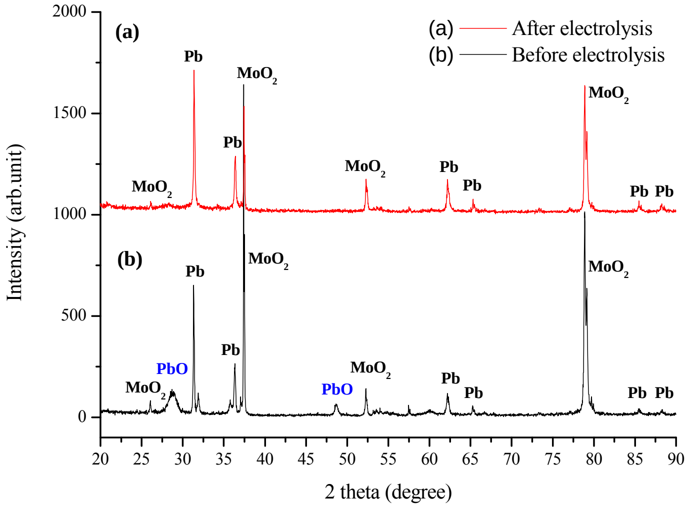

Figure S8. Powder X-ray diffraction patterns of MoO_2/Pb working electrodes. (a) After the 3 hrs of potentiostatic electrolysis under CO_2 at -2.45 V vs. Fc/Fc$^+$; (b) Before the electrolysis. Electrolyte: 0.1 M $TBAPF_6$; solvent: MeCN; temperature: -20^{o}C.

A small quantity of PbO was present initially in the sample; it was reduced during the long term electrolysis at -2.45 V vs. Fc/Fc$^+$. All the characteristic XRD peaks of MoO_2 and Pb were present in sample after electrolysis.

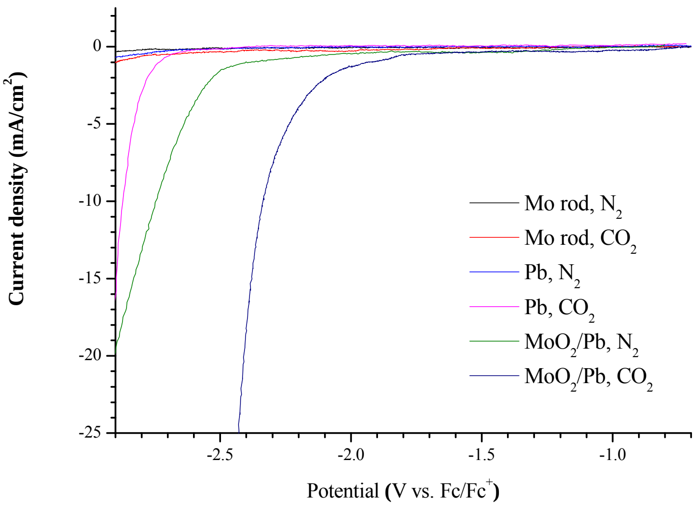

Figure S9. Polarization curves of Mo rod, Pb, and MoO_2/Pb electrodes in N_2 and CO_2-saturated MeCN at-20 °C. Electrolyte: 0.1 M $TBAPF_6$; scan rate: 50 mV/s.

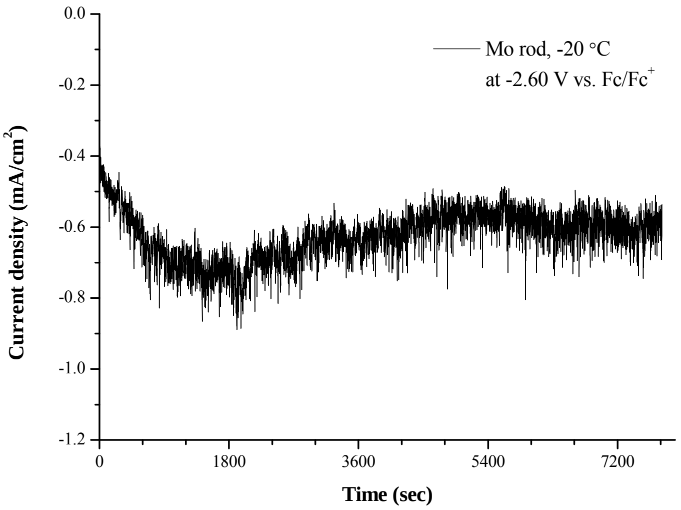

Figure S10. Potentiostatic electrolysis of Mo rod at -2.60 V vs. Fc/Fc^+ in CO_2-saturated MeCN at -20°C over 2 h. The current is negligible compared with that of MoO_2.

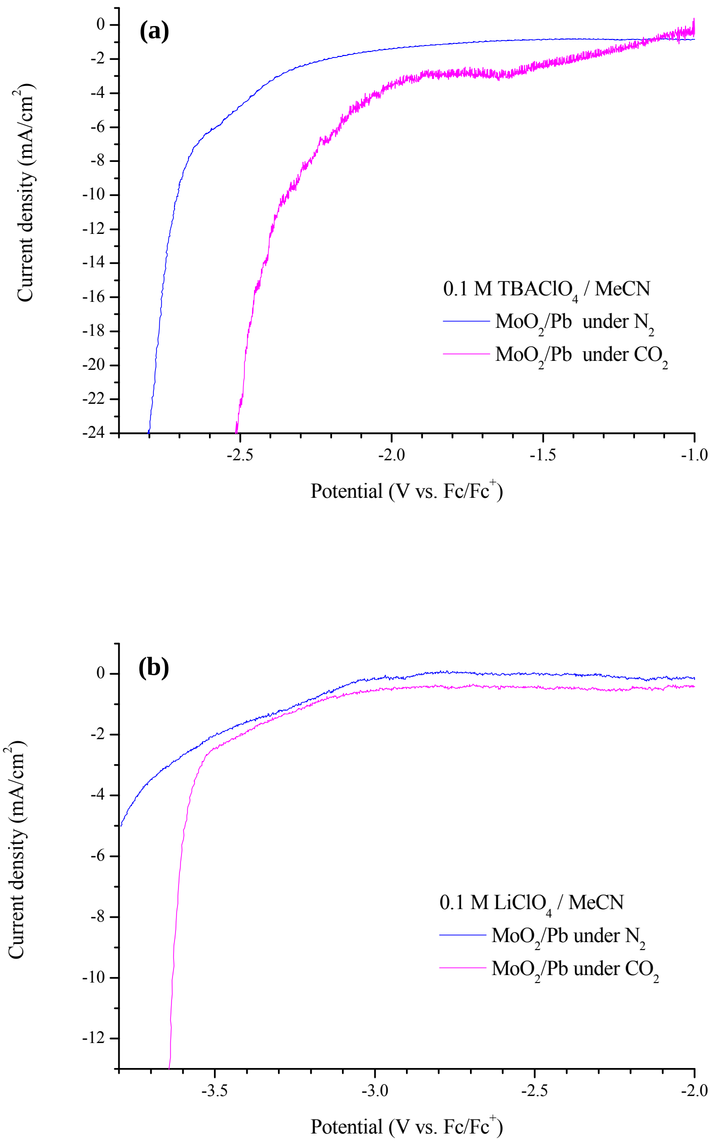

Figure S11. Polarization curves of the MoO_2/Pb electrode in N_2 and CO_2-saturated MeCN at -20 °C. Electrolyte: (a) 0.1 M $TBAClO_4$, (b) 0.1 M $LiClO_4$; scan rate: 50 mV/s.

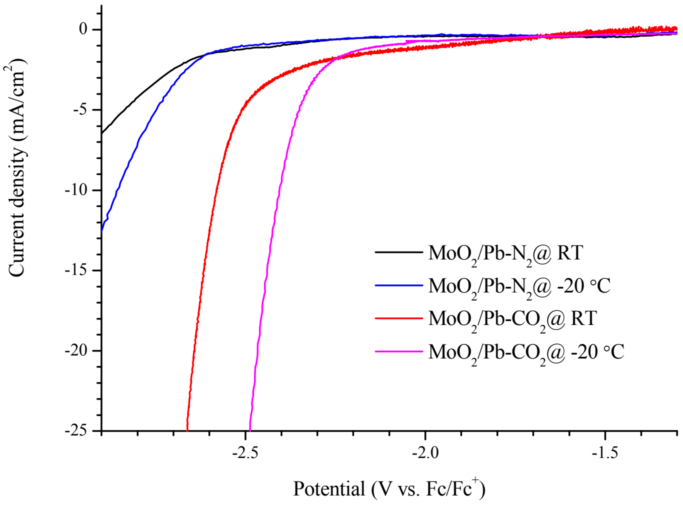

Figure S12. Polarization curves of the MoO_2/Pb electrode in N_2 and CO_2-saturated DMF at RT and -20 °C. Electrolyte: 0.1 M $TBAPF_6$; scan rate: 50 mV/s.

Electrode	Temperature (°C)	Potential (V *vs.* Fc/Fc$^+$)	Faradaic efficiency (%)				
			H_2	CO	$C_2O_4^{2-}$	$HCOO^-$	Total
MoO_2-Pb	-20	-2.30	.	9.7	11.2	.	20.9
MoO_2-Pb	-20	-2.45	.	28.1	44.2	.	72.3
MoO_2-Pb	-20	-2.60	.	30.0	44.4	.	74.4
MoO_2-Pb (0.1 M H_2O)	-20	-2.30	9.5	37.9	13.8	0.9	62.1
MoO_2-Pb (0.1 M H_2O)	-20	-2.45	3.5	33.0	37.4	0.8	74.7
MoO_2-Pb (0.1 M H_2O)	-20	-2.60	3.1	38.0	13.7	2.0	56.8
MoO_2-Pb (0.2 M H_2O)	-20	-2.30	13.4	38.3	5.5	0.4	57.6
MoO_2-Pb (0.2 M H_2O)	-20	-2.45	3.1	53.7	26	3.7	86.5
MoO_2-Pb (0.2 M H_2O)	-20	-2.60	7.5	51.5	23.2	5.6	87.8
MoO_2-Pb (0.3 M H_2O)	-20	-2.30	7.6	38.2	10.2	11.8	67.8
MoO_2-Pb (0.3 M H_2O)	-20	-2.45	10.3	55.7	17.1	10.5	93.6
MoO_2-Pb (0.4 M H_2O)	-20	-2.30	26.4	20.4	9.2	11.8	67.8
MoO_2-Pb (0.4 M H_2O)	-20	-2.45	12.4	61.6	12.4	12.5	98.9
MoO_2-Pb (0.8 M H_2O)	-20	-2.30	22.0	15.8	6.2	41.6	85.6
MoO_2-Pb (0.8 M H_2O)	-20	-2.45	19.5	13.4	9.2	49.3	91.4
MoO_2-Pb (1.4 M H_2O)	-20	-2.30	15.2	21.5	8.7	48.2	93.6
MoO_2-Pb (1.4 M H_2O)	-20	-2.45	17.5	13.1	7.8	54.4	92.8

Table S1. Faradaic efficiencies of electrocatalytic reduction of CO_2 in MeCN by the modified MoO_2-Pb electrode at -20 °C. Electrolyte: 0.1 M $TBAPF_6$. Electrolysis time: 1800 sec.

Electrode	Temperature (°C)	Potential (V *vs.* Fc/Fc$^+$)	Faradaic efficiency (%)				
			H_2	CO	$C_2O_4^{2-}$	$HCOO^-$	Total
MoO_2-Pb	21	-2.30	.	.	11.8	5.3	17.1
MoO_2-Pb	21	-2.45	.	.	11.9	39.9	51.8
MoO_2-Pb	21	-2.60	.	.	44.2	5.4	49.6
MoO_2-Pb (0.1 M H_2O)	21	-2.30	70.1	.	11.9	17.0	99.0
MoO_2-Pb (0.1 M H_2O)	21	-2.45	45.9	.	17.4	4.0	67.3
MoO_2-Pb (0.2 M H_2O)	21	-2.30	81.1	.	5.7	11.9	98.7
MoO_2-Pb (0.2 M H_2O)	21	-2.45	55.2	.	12.0	15.1	82.3

Table S2. Faradaic efficiencies of electrocatalytic reduction of CO_2 in MeCN by the modified MoO_2-Pb electrode at RT. Electrolyte: 0.1 M $TBAPF_6$. Electrolysis time: 1800 sec.

Electrode	Temperature	Potential	Faradaic efficiency (%)				
	(°C)	(V *vs.* Fc/Fc$^+$)	H_2	CO	$C_2O_4^{2-}$	$HCOO^-$	Total
Pb under N_2	21	-2.6	.	.	.	.	.
Pb under CO_2	21	-2.45	.	.	.	.	.
Pb under CO_2	21	-2.6	.	.	1.5	.	1.5
Pb under N_2	-20	-2.45	.	.	.	.	.
Pb under CO_2	-20	-2.6	.	9.3	6.7	.	16.0

Table S3. Faradaic efficiencies of electrocatalytic reduction of CO_2 by Pb electrode in MeCN at RT and -20 °C. Electrolyte: 0.1 M $TBAPF_6$. Electrolysis time: 1800 sec.

Electrode	Temperature	Potential	Faradaic efficiency (%)				
	(°C)	(V *vs.* Fc/Fc$^+$)	H_2	CO	$C_2O_4^{2-}$	$HCOO^-$	Total
MoO_2-Pb	-20	-2.30	.	15.1	12.6	51.0	78.7
MoO_2-Pb	-20	-2.45	.	40.4	16.7	41.2	98.3
MoO_2-Pb	-20	-2.60	.	45.6	26.1	25.7	97.4
MoO_2-Pb (0.1 M H_2O)	-20	-2.30	38.3	.	23.9	33.5	95.7
MoO_2-Pb (0.1 M H_2O)	-20	-2.45	7.2	32.4	31.9	3.9	75.4
MoO_2-Pb (0.2 M H_2O)	-20	-2.30	45.2	.	11.3	31.7	88.2
MoO_2-Pb (0.2 M H_2O)	-20	-2.45	26.4	18.2	17.8	14.3	76.7
MoO_2-Pb	21	-2.45	.	50.0	8.6	41.1	99.7
MoO_2-Pb	21	-2.60	.	54.3	18.7	25.3	98.3
MoO_2-Pb (0.1 M H_2O)	21	-2.45	45.1	20.7	5.7	27.8	99.3
MoO_2-Pb (0.1 M H_2O)	21	-2.60	30.8	22.3	19.4	20.1	92.6

Table S4. Faradaic efficiencies of electrocatalytic reduction of CO_2 by the MoO_2/Pb electrode in DMF at RT and -20 °C. Electrolyte: 0.1 M $TBAPF_6$. Electrolysis time: 1800 sec.

Electrode	Electrolyte	Temperature	Potential	Faradaic efficiency (%)				
		(°C)	(V *vs.* Fc/Fc$^+$)	H_2	CO	$C_2O_4^{2-}$	$HCOO^-$	Total
MoO_2-Pb	0.1 M $TBAClO_4$	-20	-2.45	.	45.6	.	53.8	99.4
MoO_2-Pb	0.1 M $TBAClO_4$	-20	-2.60	.	41.6	18.3	29.2	89.1
MoO_2-Pb	0.1 M $LiClO_4$	-20	-2.45	.	.	.	.	.
MoO_2-Pb	0.1 M $LiClO_4$	-20	-3.80	.	.	.	46.0	46.0

Table S5. Faradaic efficiencies of electrocatalytic reduction of CO_2 by the MoO_2/Pb electrode in MeCN at -20 °C. Electrolyte: 0.1 M $TBAClO_4$ and 0.1 M $LiClO_4$. Electrolysis time: 1800 sec.

Reference:

1. J. Zhou, N. S. Xu, S. Z. Deng, J. Chen and J. C. She, *Chem Phys Lett*, 2003, **382**, 443-446.
2. R. R. Gagne and D. M. Ingle, *J. Am. Chem. Soc.*, 1980, **102**, 1444-1446.
3. G. Gritzner and J. Kuta, *Pure Appl Chem*, 1984, **56**, 461-466.